MecSol2013
International Symposium on Solid Mechanics
April 18-19, 2013
Porto Alegre, Rio Grande do Sul, Brazil

An inverse methodology for tuning material parameters in numerical modeling of mechanical structures

Miguel Angel Calle Gonzales
Group of Solid Mechanics and Structural Impact
Department Mechatronics and Mechanical Systems
Polytechnic School of the University of Sao Paulo, SP, Brazil
mcallegonzales@gmail.com

Marcílio Alves
Group of Solid Mechanics and Structural Impact
Department Mechatronics and Mechanical Systems
Polytechnic School of the University of Sao Paulo, SP, Brazil

ABSTRACT

Codes for numerical modeling of structures are of vital importance in the engineering practice. Finite element analysis can predict the response of complex components and structures, reducing the costs of experimental programs. However, among other aspects, the accuracy of the material input parameters in the model underlines the efficacy of the modeling to represent an actual event. In this work the mechanical properties extracted from a conventional uniaxial tensile test, using the traditional procedure and digital image correlation technique, are used in a simple numerical model. The correspondence between the numerical model and one experimental test is found to be not as good as it were expected. This is due to the difficulty of analyzing the raw data after necking. An inverse technique is then proposed by adjusting the numerical model to the experimental response to find the optimal and most representative material parameters. This methodology was implemented in a finite element code with the support of an iterative routine. A comparative analysis of the results and a brief discussion about material failure and element size effects is also presented.

Keywords: tensile test, mechanical properties, inverse methodology.

1 INTRODUCTION

Uniaxial tensile test on standard samples is broadly used in research and in industrial applications to obtain mechanical properties of materials. Practical methodologies for obtaining the stress strain curve from a uniaxial tensile test are generally standardized for industrial applications. These methodologies give valuable information to meet industrial requirements but are somewhat restricted for scientific investigations.

In tensile samples, after necking formation, the information obtained is somewhat limited due to difficulties in measuring experimentally local stresses and strains. Some investigations raised in the last years to overcome these practical limitations by correcting the material curve based in empirical data [1-5] and, in some way, improving other more traditional studies about correcting material curve in circular section specimens [6-7].

Based on experimental and numerical analyses, Mirone [1] detected a recurring pattern in the nonhomogeneous stress field in the necking zone, which is nearly material independent. This

perturbing effect was quantified in [1] and used to correct true stress strain curves obtained from uniaxial tensile tests of round section specimens, giving more accurate results for the material equivalent stress than the Bridgman method [6].

In recent years, non-contact photogrammetric techniques as the Digital Image Correlation (DIC) became powerful experimental tool for measuring strains field directly in the specimen. Other authors as Kamaya and Kawakubo [2] developed a progressive iteration process to obtain the true stress strain curve, point by point from low to higher strain values. A numerical modeling of a uniaxial tensile test was used in the iteration process in which the resulting force-axial strain curve was compared to an experimental reference. The DIC technique was employed in the acquisition of specimen geometry variables during the test as, for example, the minimum radius in the neck of the round section specimen. Good agreement was achieved using this iteration process.

Due to the large use of sheet material in industry, some researchers studied how to obtain equivalent true stress strain curves from uniaxial tensile tests of sheet specimens. These methods are complex to implement because in some cases it requires devices to measure parameters such as width and thickness during the tests [3-4], or iterative routines based on analytical formulations of the plasticity theory [5]. On the other hand, inverse methods have been used recently in the identifications of material parameters from experimental data [8].

In the first part of this work, a uniaxial tensile test was analyzed to obtain the stress strain curve and the maximum plastic strain of the material using these methodologies. In the second part, the material failure parameters were evaluated by using an inverse methodology for various element mesh sizes. A formulation to correlate the influence of the element size on the maximum plastic strain was proposed.

2 EVALUATION OF THE STRESS STRAIN CURVE

In a uniaxial tensile test, force, F, is measured by a load cell mounted in a universal test machine. As for strains, they are acquired directly from the machine frame displacement, ΔL, or by using external strain gauges mounted directly on the specimen. Optical clip gages are also available, they track targets in the specimen. These procedures allow the calculation of the engineering strain, e, and the engineering stress, S,

$$e = \frac{L - L_0}{L_0} = \frac{\Delta L}{L_0} \tag{1}$$

$$S = \frac{F}{A_0} \tag{2}$$

from which the true stress, σ, and true strain, ε, are estimated by:

$$\varepsilon = \int_{L_0}^{L} \frac{dL}{L} = \ln\left(\frac{L}{L_0}\right) = \ln(1 + e) \tag{3}$$

$$\sigma = \frac{F}{A} = S\frac{A_0}{A} = S\frac{L}{L_0} = S(1 + e) \tag{4}$$

Here, uniaxial tensile test were carried out on mild steel (SAE 1006) in an Instron universal machine at a constant velocity of 0.2 mm/min. The specimen was extracted from a steel plate coil in the rolling direction with an initial length of 80 mm and an initial section of 12 mm × 1 mm. The force was acquired by the load cell of the universal machine at a frequency of 2 Hz and the strain by

a non-contact photogrammetric technique called Digital Image Correlation (DIC). Digital images were recorded along the entire test with a frequency of one image every five seconds (0.2 Hz). The surface of the specimen was previously painted with white and speckled with black ink to form a black and white random pattern in order to allow the use of the DIC technique, Fig. 1. A Nikon D90 digital camera was employed and the images were taken in TIFF format with a size of 2848 × 4288 pixels so giving a 70 MB size each photo, Fig. 1. A LED lightning system was also used in the acquisition of the images so allowing a faster shutter speed.

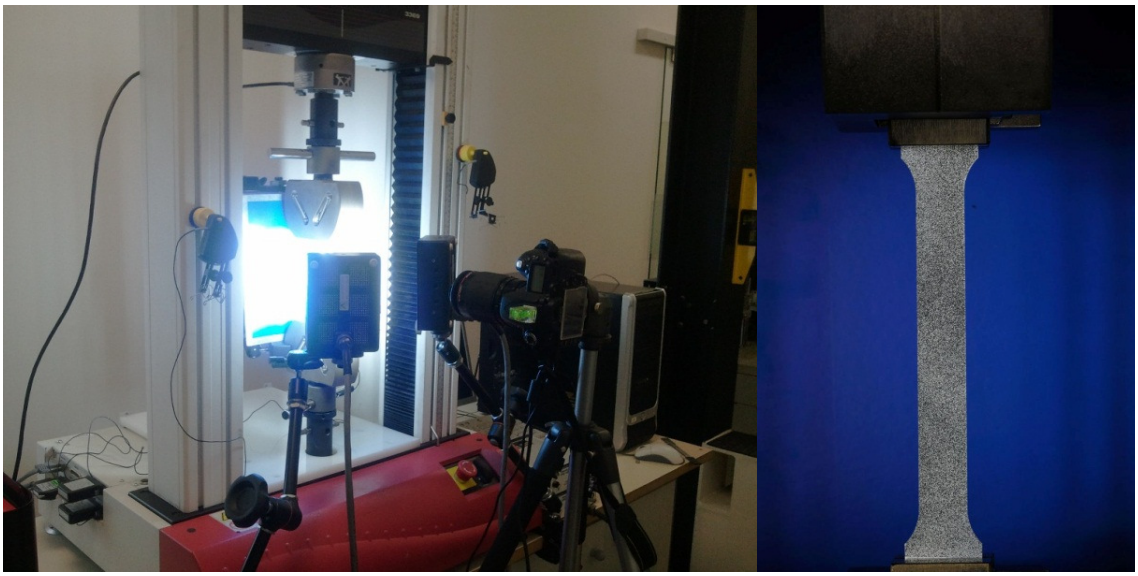

Figure 1: Acquisition of the images during the tensile test and image acquired.

Five methods were used to evaluate the true stress strain curve of the tested material: measurement obtained directly from the universal machine, by using an external clip gage, by tracking displacement of two points, using DIC analysis and using the inverse methodology.

The evaluation of the stress strain curve can be done by using the displacement of the machine crosshead (ΔL) to calculate the true strain and true stress of the material using the equations mentioned above. This method is somewhat limited because deformations in machine clamps, tightening, sliding among others mechanical adjustments can influence the measurement. Alternatively, when an external clip gage is mounted on the specimen or optical techniques are used to acquire relative displacements of two points in the specimen surface, the true strain history during the test can be acquired directly from the measurement apparatus. The principal limitation of these measurement techniques is that the measured strain history within the gauge length is only valid prior localization. On the other hand, the whole strain field, even after localization, i.e. when necking takes place, can be accurately measured using DIC, as illustrated in Fig. 2.

Here, the DIC method was performed using the software 7D developed by Valcher et al. [9] to acquire the strains field in the frontal surface of the specimen, as it can be seen in Fig. 2. The 7D software distinguishes the strains evolution in the surface of the specimen by recognizing the displacement and distortion of the black and white pattern in the images. As shown in Fig. 2, a grid of 45 × 90 elements, grid size of 8 × 8 pixel and a pattern size of 16 × 16 were initially used to evaluate the strains field. It can be interpreted as a mesh with element size of about 0.26 mm × 0.26 mm over an area of 12 × 24 mm in the surface of the specimen. A shear failure was detected in the specimen by the angle between the fracture surface and the load direction, see Fig. 2.

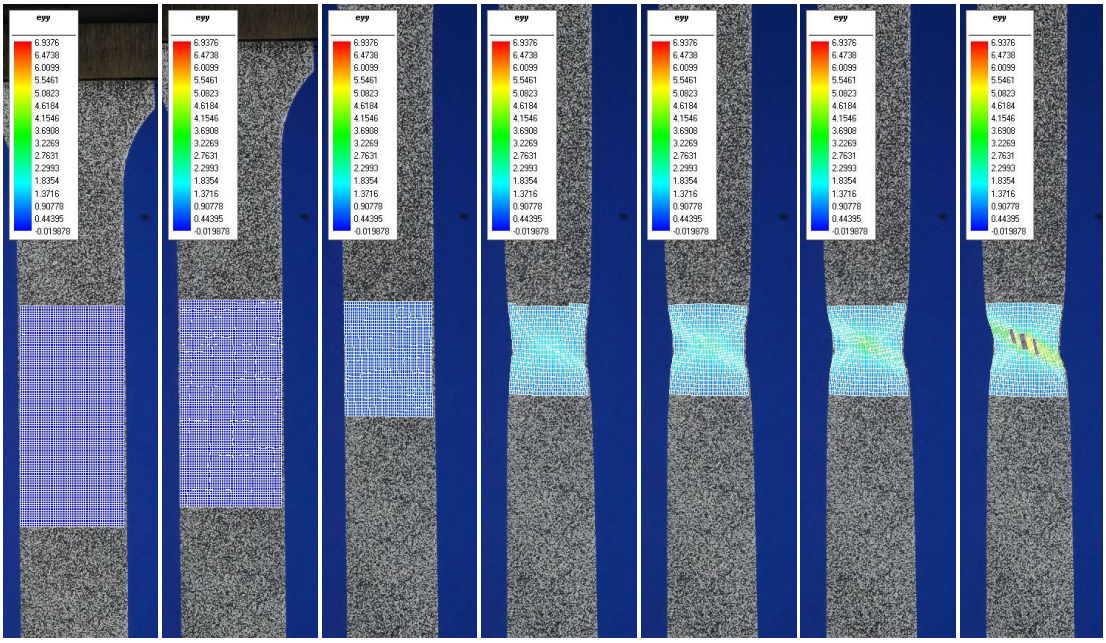

Figure 2: Digital image correlation analysis of the tensile test

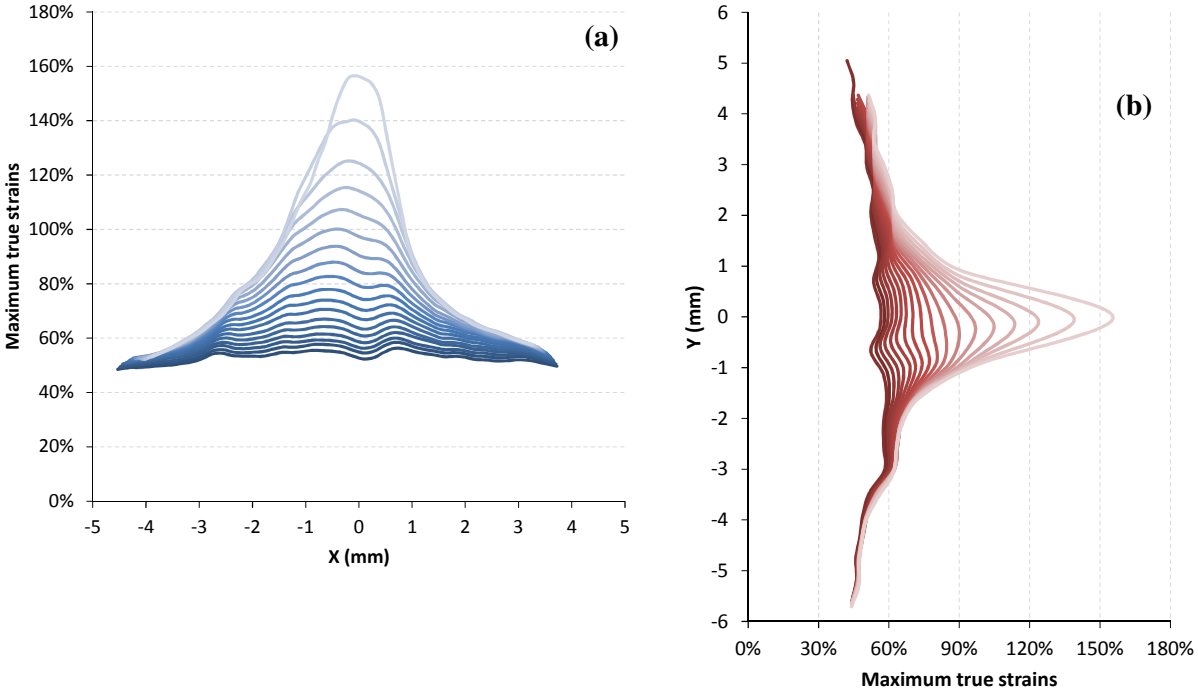

Figure 3: Analysis of the strains distribution along the (a) horizontal section of failure and (b) the vertical axis after the necking point.

In the analysis of the results, three stages can be identified during the tensile test: elastic regime, plastic regime before and after necking. During the elastic and plastic regimes before necking, the specimen experiences a uniform strain. But this behavior changes after the necking point: different strain evolution depending of the distance from the vertical center line of the

specimen, Fig 3a. Hence, the middle point in the specimen achieves a maximum strain until failure thus, probably, indicating the origin of the crack.

Fig. 3a shows the strain history in the necking cross section of the specimen. It is observed that the distributions of strains, after the necking point, modify from a regular plain distribution of strains to a concentration of highly strained material in the middle of the section so giving a difference higher than 100% strain when compared with strain in the edge of the section. In addition, Fig. 3b shows the strain history distribution along the length of the specimen. It is possible to observe strain values in this region some three times larger than the strain values in regions outside necking.

For the estimation of the true stress strain curve using the DIC technique, average true stress and strain values over all the necking cross section of the specimen was considered. It was also assumed that the strains along the thickness of the specimen do not change, in contrast with Figure 3. The average true stress was based in the actual force acquired by the load cell of the machine divided by the actual area in the necking section. This actual area is defined as the width of the specimen in the neck multiplied by its actual thickness ($W \times T$). The width was obtained by tracking the displacement of both edge points in the minimum section using the DIC technique (considering uniform transversal deformation) and the thickness of the section was calculated assuming Volume Conservation (VC) in plastic regime. It follows that:

$$\varepsilon^{DIC} = \frac{1}{n}\sum_{i=1}^{n} \ln\left(1 + e_{yy}^{DIC}\right) \tag{5}$$

$$\sigma^{DIC} = \frac{F}{W^{DIC}.T^{VC}} \tag{6}$$

$$Vol = W_0\, T_0\, L_0 = W^{DIC}\, T^{VC}\, L^{DIC} \tag{7}$$

$$T^{VC} = \frac{W_0\, T_0 L_0}{W^{DIC}\, L^{DIC}} \tag{8}$$

Although the above procedure averages the strains, it is similar to what could be obtained with the use of strain gauges in the necking zone.

An inverse methodology was developed for obtaining the material parameters of the analyzed material. This methodology is defined as the adjustment of the numerical model response to the analogous experimental response of a mechanical test. This adjustment is based in the fine tuning of certain parameters of the numerical model to attain the desirable response mentioned above. This fine tuning is generally achieved by using an optimization methodology. In this case, the material parameters are adjusted so that the numerical model of the uniaxial tensile gives nearly the same force-displacement response as the experimental test. The experimental force displacement response was acquired considering the force from the load cell of the machine and the displacement within two points, set apart 50 mm and centered in the length of the specimen, which equals the clip gage set up. The inverse methodology procedure was developed by using two commercial codes. The Matlab software was used for the optimization routine and the Ansys code for the Finite Element (FE) numerical models processing. The diagram shown in Fig. 4 explains the procedure to adjust the material parameters.

A tridimensional FE model of the tensile test was developed considering an implicit analysis, symmetry in the geometry along the length of the specimen, a constant loading curve, equivalent to the experimental test and the elastic plastic behavior of the material, Fig. 5. The element size in the

middle of the specimen was a regular 0.25 mm side cube. The Voce material model was chosen because this material model describes the plastic behavior of the material by employing four parameters.

$$\sigma = k + R_0 . \varepsilon + R_\infty (1 - e^{-b\varepsilon}) \tag{9}$$

where k is the yield stress, obtained directly from the experimental test, and the others three variables (R_0 , R_∞ and b) needed to be adjusted by the optimization routine. The resultant parameters adjusted by the optimization procedure were presented in Table 1. The optimization loop ends when the integral of the area between experimental and numerical force - displacement curves (error)

$$min\left\{\sum_{i=1}^{n}\left|F_i^{exp} - F_i^{num}(R_0, R_\infty, b)\right|\left(\frac{d_{i+1} - d_{i-1}}{2}\right)\right\} \tag{10}$$

attains a minimum value. The Voce material parameters obtained by this optimization methodology are shown in Table 1, including the Maximum True Equivalent Plastic Strain value (MPS) in which failure takes place.

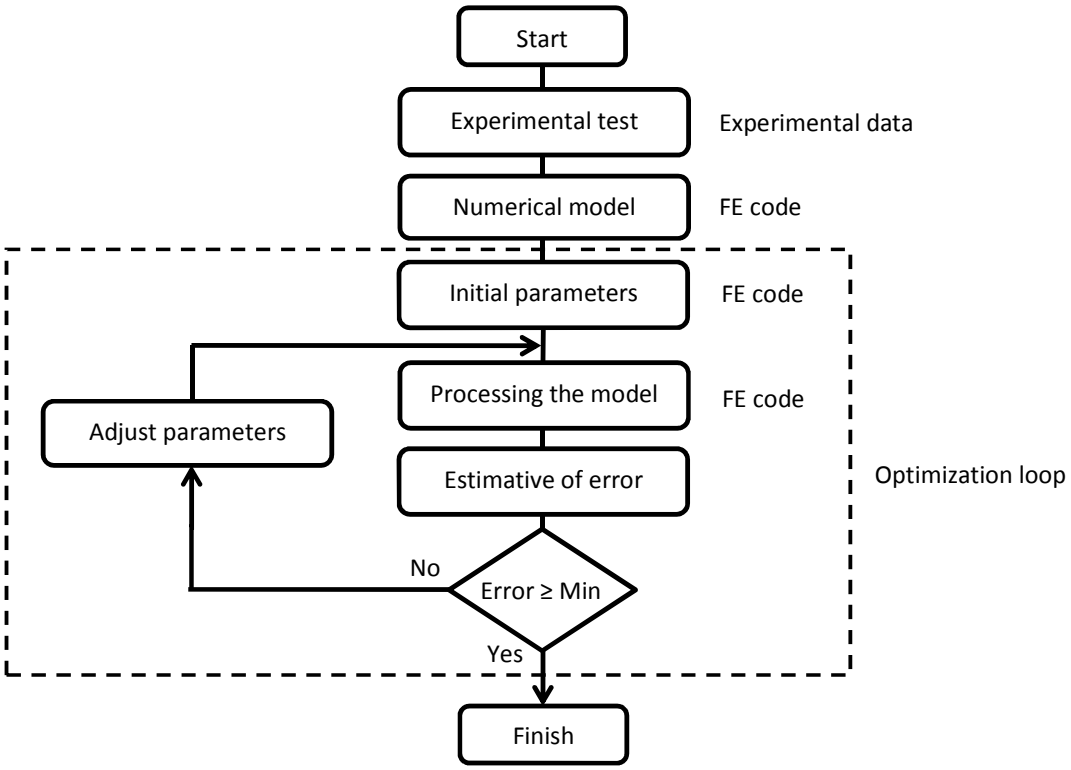

Figure 4: Diagram of inverse methodology to adjust material parameters.

Table 1. Material parameters obtained by the inverse methodology.

Voce parameter k	157.6 MPa
Voce parameter R_0	392.0 MPa
Voce parameter R_∞	133.1 MPa

Voce parameter b	28.38
Maximum Plastic Strain (MPS)	171.2%

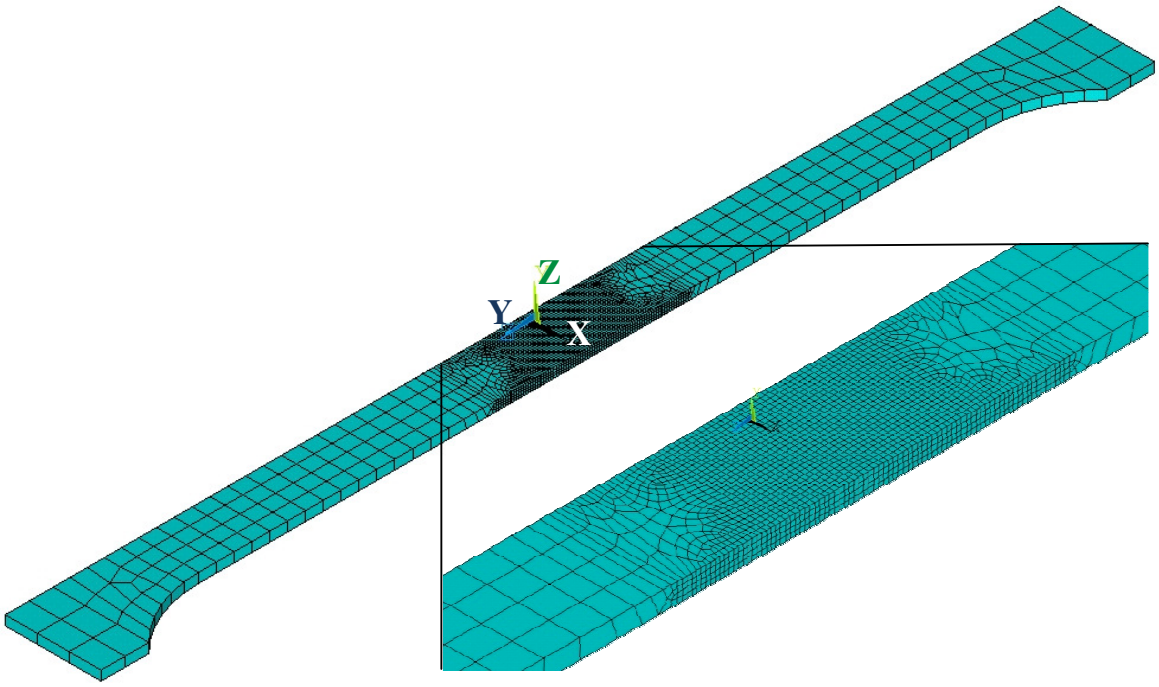

Figure 5: Tridimensional model of half specimen of tensile test and detail of the central area.

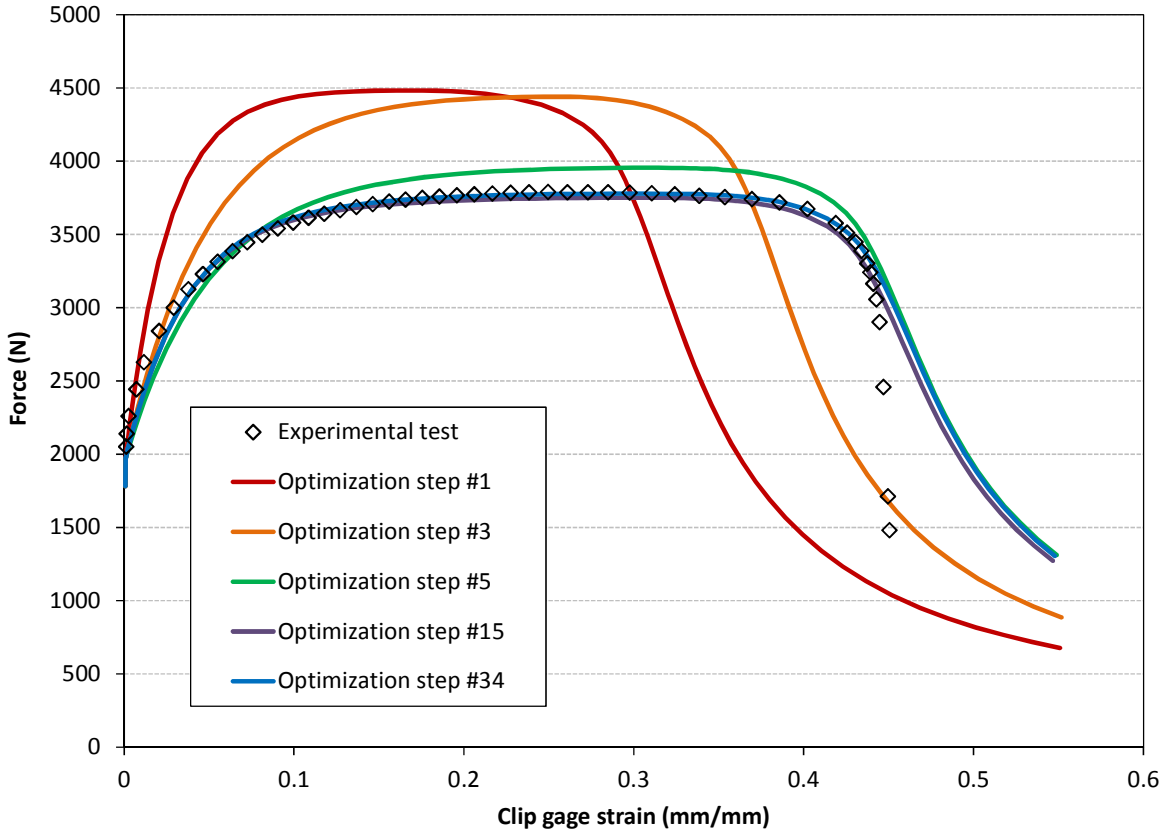

Figure 6: Comparison of the stress strain curves obtained by five different methods.

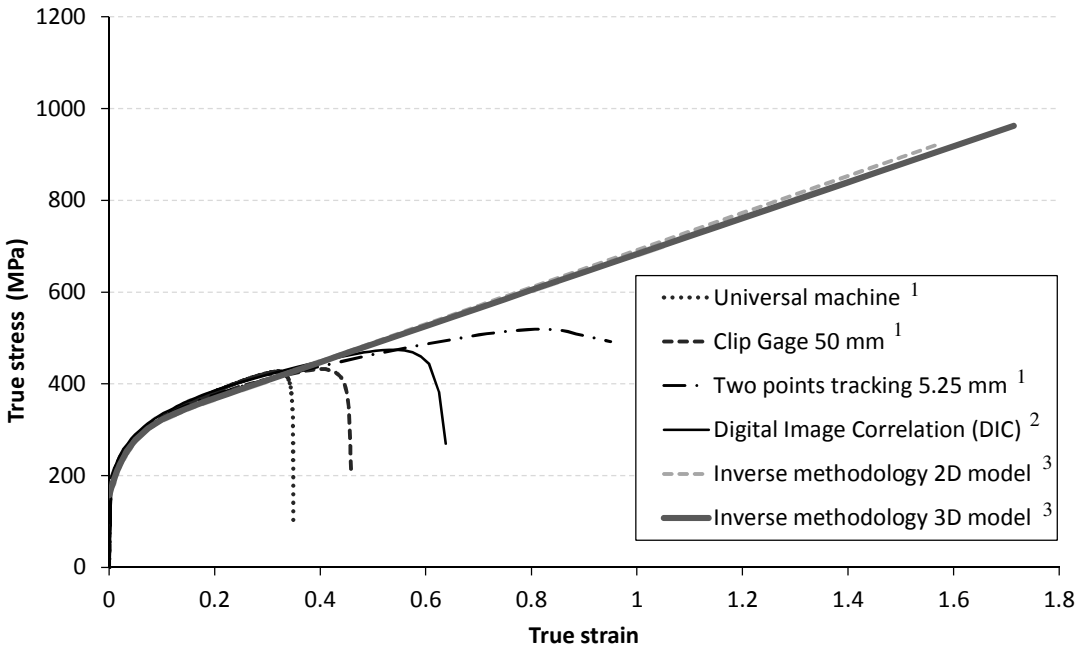

Figure 7: Comparison of the stress strain curves obtained by five different methods.

[1] Curves obtained from equations (1), (2), (3) and (4). [2] DIC curve obtained from average stress and strain in the y direction on the cross section failure area of the specimen. [3] Equivalent stress strain curve from FE analysis.

Partial force – clip gage strains from the optimization routine were shown in Fig. 6 for the tridimensional FE model. The complete optimization procedure required 34 steps.

The true stress strain curves from the five methods here discussed are presented in Fig. 7.

The limitations of various procedures are clearly shown. As commented before, the evaluation of the strain using two reference points in the length of the specimen is limited to the moment where the necking begins. As necking initiates, the strain distribution in the section of the specimen is no longer uniform and the strain history will not represent the local plastic behavior. Even using the displacement of the machine crosshead, a clip gage or two points tracking at any relative distance, the estimated curve will stop following the actual stress strain curve. By using the DIC technique, it is possible to widen the extent of the stress strain curve acquisition to values close to twice the strain range. Since the DIC technique is limited to the number of photos acquired, strain evaluation is limited to the strain field on the surface of the specimen and the maximum distortion of the pattern painted in the specimen surface. The DIC technique did not capture the entire stress strain curve until the failure point. On the other hand, the inverse methodology permits to obtain the entire stress strain curve until complete failure thanks to the fine tuning of the material parameters.

3 ANALYSIS OF ELEMENT SIZE EFFECT ON MATERIAL PARAMETERS

When a numerical model is developed to simulate a structural test or event, the element mesh size is usually different depending on the structure geometry, so requiring more refined mesh in

areas with loading application, contact, stress concentration and so on. The material parameters can be affected by different element mesh sizes [10]. As a further study, mechanical properties of the material tested were estimated using the inverse methodology with different element mesh sizes, Fig. 8. Bi-dimensional models were submitted to the optimization procedure using as input data the force - clip gage strain curve obtained experimentally (clip gage of 50 mm length). The Voce material parameters were estimated similarly as seen previously in the tridimensional model.

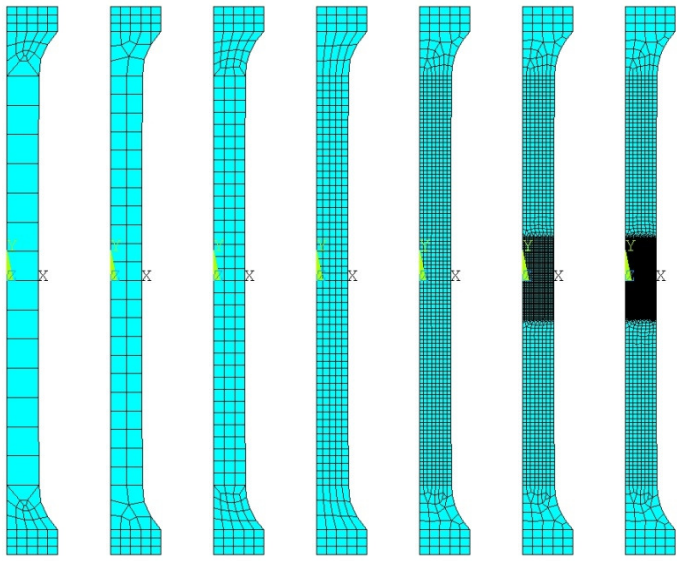

Figure 8. Meshes for tensile test models using different element sizes.

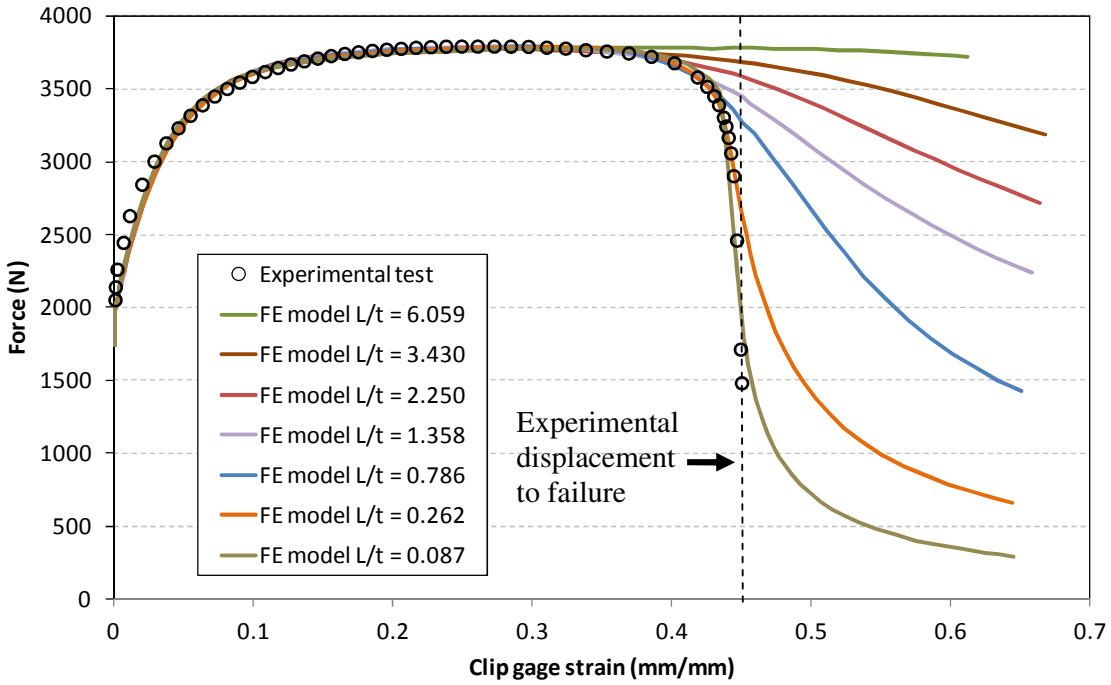

Figure 9: Force strain curves obtained from experimental test and FE models (without considering failure criterion) using different element mesh sizes.

Fig. 9 shows the resultant force - clip gage strains curves for specimens with different thickness ratios (element size divided by thickness), without considering a failure criterion in the models. It can be observed that the more refined numerical model represents better the experimental reference. The results suggest a tendency for a better adjustment of the numerical response to the experimental reference, as the element mesh size decreases. It justifies the abrupt rupture of the specimen once it reaches a certain plastic strains requirement as seen in the experimental test, so explaining the falling in the force-clip gauge strain curve near failure. This is here attributed to the stress strain curve and not caused by factors as damage of the material near failure. Also, it was observed that the resultant stress strain curves, for different mesh sizes obtained in the optimization routine, show no significant difference, at least until their failure limit.

When the displacement in the numerical model reaches the actual displacement to failure, failure is said to occur. So no coupling is here considered. Most severe stress states and maximum plastic strains were detected in the center of the middle section of the specimen, as expected. Failure analysis was developed in this critical point of the specimen. Fig. 10 shows the maximum equivalent plastic strain just before failure, which also shows a decreasing of the maximum plastic strain at failure when increasing the dimensionless mesh size (element mesh size divided by the thickness). This is known as mesh size effect on failure strain.

Several formulations were created to correlate the maximum plastic strain (or the failure parameter when using another failure criterion) with the dimensionless mesh size when analyzing plate structures [11-13]. Here, it was analyzed the element size effect on four different failure criteria. The first failure criteria reviewed was the equivalent plastic strain, which is heavily used due to its simplicity and broad availability in most of the commercial finite element codes. The other criteria can be classified as empirical models, with failure considered to occur when an integral of $f(\sigma, \varepsilon)$, which depends on the history of the stress and strain states, reaches a critical value. The second failure criterion was proposed by Freudenthal [14] based on strain energy density, $\int_0^{\bar{\varepsilon}_f} \bar{\sigma} d\bar{\varepsilon} = C$. The third is the Cockcroft-Latham criterion [15] based exclusively on the principal stress history, $\int_0^{\bar{\varepsilon}_f} \sigma_1 d\bar{\varepsilon} = C$. The fourth was proposed by Ayada et al. [16] based on the history of the triaxiality parameter defined by the hydrostatic stress divided by the equivalent Von Mises stress, $\int_0^{\bar{\varepsilon}_f} \frac{\sigma_h}{\bar{\sigma}} d\bar{\varepsilon} = C$.

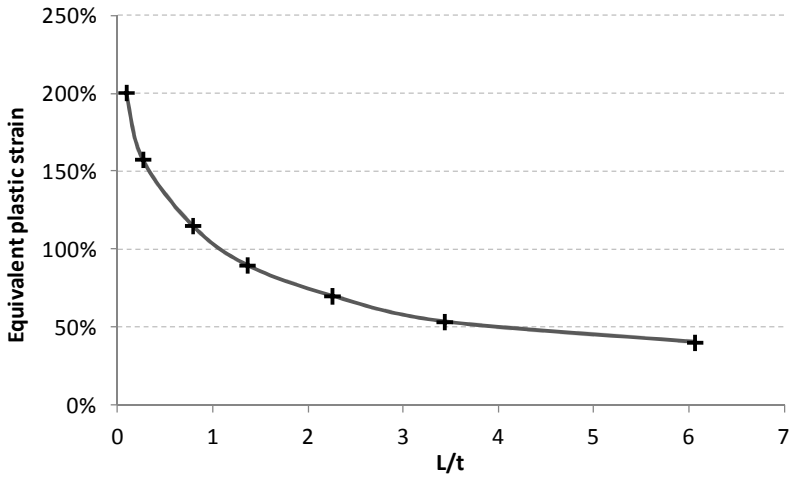

Figure 10: Influence of the element mesh size on the maximum plastic strain.

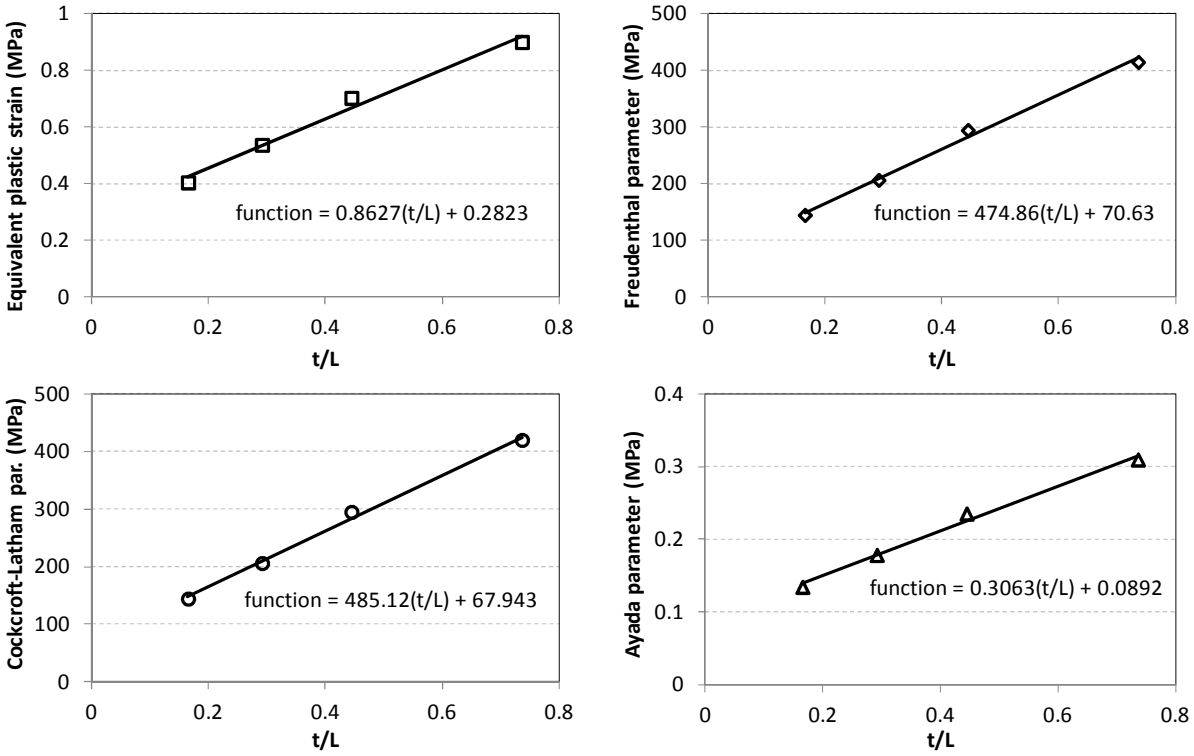

Figure 11: Influence of the element size on critical parameter of the failure criteria.

Here, only the models with L/t > 1 were analyzed so avoiding shell elements with dimensions smaller than its thickness. In Fig. 11 the critical parameter for each criterion was estimated considering different element sizes. A linear relation between the critical parameters for all the criteria analyzed with the inverse of the thickness ratio (*L/t*) value was found. So, the formulation to evaluate the material failure can be redefined as below to include the element size effect with *A* and *B* listed in Table 2 being mesh dependent material parameters,

$$function = \int_0^{\bar{\varepsilon}_f} f(\sigma, \varepsilon) d\bar{\varepsilon} = A\left(t/L\right) + B \qquad (11)$$

Table 2. Parameters of Eq.(11) for four different failure criteria.

FAILURE CRITERIA	*A*	*B*
Equivalent plastic strain	0.8627	0.2823
Freudenthal	474.86 MPa	70.63 MPa
Cockcroft-Latham	485.12 MPa	67.943 MPa
Ayada	0.3063	0.0892

4 CONCLUSION

The inverse methodology here used proved to be a powerful technique to obtain the mechanical properties of the material from an experimental uniaxial tensile test. The results showed

a major competence of the inverse methodology when compared to DIC technique because it is not required an experimental scheme for image acquisition or software for photogrammetric analysis of the strains field. Conversely, the inverse methodology requires a FE code and programming software to elaborate the optimization routine. A remarkable dependence of the failure criteria on the element size was found and a formulation was proposed to take into account this dependence when shell elements are used.

REFERENCES

[1] Mirone, G., 2004, 'A new model for the elastoplastic characterization and stress-strain determination on the necking section of a tensile specimen'. International Journal of Solids and Structures, V.41, pp.3545-3564.

[2] Kamaya, M. and Kawakubo, M., 2011, 'A procedure for determining the true stress–strain curve over a large range of strains using digital image correlation and finite element analysis'. Mechanics of Materials, V.43, pp.243-253.

[3] Bacha, A., Daniel, D. and Klocker, H., 2007, 'On the determination of true stress triaxiality in sheet metal'. Journal of Materials Processing Technology, V.184, pp.272–287.

[4] Zhang, Z. L., Ødegård, J. and Søvik, O. P., 2001, 'Determining true stress-strain curve for isotropic and anisotropic materials with rectangular tensile bars: method and verifications'. Computational Material Science, V.20, pp.77-85.

[5] Joun, M., Eom, J. G. and Lee, M. C., 2008, 'A new method for acquiring true stress–strain curves over a large range of strains using a tensile test and finite element method'. Mechanics of Materials, V.40, pp.586-593.

[6] Bridgman, P. W., 1956, 'Studies in large flow and fracture'. McGraw-Hill.

[7] Alves, M. and Jones, N., 1999, 'Influence of hydrostatic stress on failure of axisymmetric notched specimens'. J. Mech. Phys. Solid, V.47, pp.643-667.

[8] Pottier, T., Toussaint, F. and Vacher, P., 2008, 'An inverse method for material parameters determination of titanium samples under tensile loading'. International Journal of Metal Forming, v.1, n.1, pp.21-24.

[9] Valcher, P., Dumoulin, S., Morestin, F. and Mguil-Touchal, S., 1999, 'Bidimensional strain measurement using digital images'. Proc. Institution of Mech. Engineers, n. 213, p. 811-817.

[10] Ehlers, S. and Varsta, P., 2009, 'Strain and stress relation for non-linear finite element simulations'. Thin-Walled Structures, Vol.47, pp.1203-1217.

[11] Yamada, Y., Endo, H. and Pedersen, P.T., 2005, 'Numerical study on the effect on buffer bow structure in ship-ship collision', Proc. 15th Int. Offshore and Polar Engineering Conference.

[12] Peschmann, J. and Kulzep, A., 2000, 'Side collision of double skin ships'. BMBF report, Tech. Univ. Hamburg.

[13] Scharrer, M., Zhang, L. and Egge, E.D., 2002, 'Collision calculations in naval design systems'. Report, Germanischer Lloyd, Hamburg.

[14] Freudenthal, A.M., 1950, 'The inelastic behavior of solids'. Ed. Wiley, New York.

[15] Cockcroft, M. G. and Latham, D. J., 1968, 'Ductility and the workability of metals'. J.Inst.Met. V.96, pp.33-39.

[16] Ayada, M., Higashino, T. and Mori, K., 1987, 'Central bursting in extrusion of inhomogeneous materials'. Advanced technology of plasticity lange, K. Springer-Verlag, Berlin, pp 553-558.